Thermochimica Acta, 18 (1977) 73–94

DIRECT ANALYSIS OF POLYMER PYROLYSIS USING LASER MICROPROBE TECHNIQUES*

R. M. [illegible]
Bell Laboratories, Murray Hill, N.J. 07974 (U.S.A.)

ABSTRACT

A laser microprobe–mass analysis technique has been developed which enables the overall course of polymer decomposition processes to be directly followed. Volatile pyrolysis products evolved during laser-vaporization of the polymer substrate are immediately formed into a molecular beam and mass analyzed. Modulated molecular beam techniques are utilized to provide increased detection sensitivity and to aid in the analysis of complex mass spectra by providing a means to directly discriminate parent ions from fragment ions. Elimination of intermediate product collection stages permits the time-resolved behavior of the polymer decomposition process to be investigated. Results are presented for rigid and plasticized polyvinyl chloride, a polyoxymethylene copolymer and a polyester elastomer block copolymer.

INTRODUCTION

In the pyrolysis of organic polymers extensive breakdown of the sample into a large number of low-molecular-weight volatile species usually occurs. Interaction of these species in the gas phase, with the hot walls of the pyrolysis chamber, and even with the sample itself can result in the generation of secondary products. The identity of reactive species is not preserved and the primary pyrolysis reactions which initiate thermal degradation are effectively masked. Elimination of secondary reactions requires remote location of the heat source, selective heating of the sample material alone, and immediate withdrawal and analysis of the volatile products.

Initial experiments on polymer degradation induced by radiant sources employed xenon flash lamps coupled with mass analysis of the evolved species[1,2]. In the technique devised by Friedman[1], analysis was complicated by insufficient control of the energy source and location of the flash lamp in the reaction chamber of the mass spectrometer. With the development of the laser and use of intense focused beams these problems were overcome. However, most studies on the interaction of laser radiation with matter have concentrated on inorganic

*Presented at 6th North American Thermal Analysis Society Conference, Princeton, N.J., June 20–23, 1976.

materials; reviews are given by Honig[3] and Knox[4]. The advantages of laser probe–mass analysis for the investigation of the pyrolysis reactions which control polymer degradation have not been fully utilized. Early work by Joy and Reuben[5] was plagued by: (1) difficulties in discriminating between evolution of adsorbed gases and true polymer decomposition species; and (2) uncertainty as to whether observed ions were produced by simple ionization of pyrolysis products or by fragmentation of parent molecules during electron bombardment. More recent work[6,7] has emphasized the microanalysis aspect of the technique for detection of inclusions and trace contaminants in polymers.

This paper introduces the technique of laser probe–molecular beam sampling and phase spectrometry to the thermal analysis of polymer materials. Volatile pyrolysis products evolved during laser-vaporization of the polymer substrate are immediately formed into a molecular beam which is mechanically chopped and mass analyzed. Phase lags develop between the various modulated ion signals as a result of the different velocities characteristic of each species in the molecular beam. This information is the basis of the phase spectrometry technique which enables parent ions of pyrolysis products to be distinguished from fragment ions created in the ion source. Molecular beam sampling eliminates intermediate product collection stages and permits the overall course of the thermal decomposition process to be directly followed. Time-resolved signals provide information on the evolution characteristics of the volatile species. Release of adsorbed gases can be identified by differences exhibited in the character of the evolution profiles. The influence of polymer additives on the decomposition process is examined through their effects on the composition and relative vaporization rates of the volatile species. Results are reported for rigid and plasticized polyvinyl chloride, a polyoxymethylene copolymer and a polyester elastomer block copolymer.

EXPERIMENTAL TECHNIQUE

A schematic of the laser probe–molecular beam apparatus is shown in Fig. 1. Relatively low power cw lasers with spectral outputs in the visible (argon-ion laser, $\lambda = 514.5$ nm) and infrared regions (CO_2 laser, $\lambda = 10.6\,\mu$m) are used to probe the polymer samples. A lens is used to focus the laser radiation onto the sample. The laser beam intensity at the sample surface can be varied from 10–1000 W cm^{-2} with both sources by changing the lens-to-sample distance. Laser pyrolysis places no special requirements on sample handling procedures and thus laser target samples of various geometries can easily be examined. In the present experiments all polymer materials were formed into specimen disks of 0.5 mm thickness. Typical sample weights prior to irradiation range from 30–50 mg.

The sample cell is directly coupled to the inlet of the mass spectrometer system via a 0.5 mm diameter orifice, and is evacuated through this orifice by

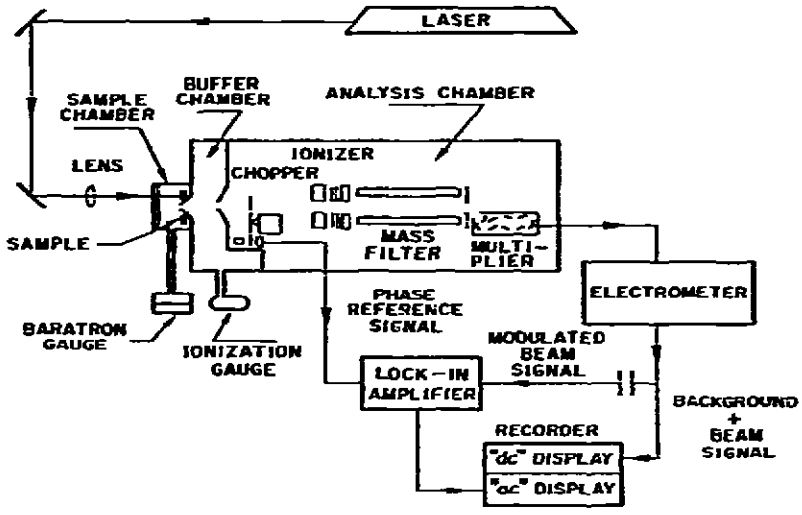

Fig. 1. Schematic of laser probe–molecular beam apparatus.

the buffer chamber pump. Upon laser irradiation a plume of volatile products is generated from the polymer surface, immediately formed into a molecular beam, ionized by electron impact (70 eV electron energy) and analyzed with a quadrupole mass filter. Prior to ionization the molecular beam is modulated with a mechanical chopper located in the analysis chamber. Standard synchronous detection techniques are used to separate the desired molecular beam signal from the unmodulated background signals resulting from residual gases always present in the analysis chamber. Background subtraction techniques are obviated and identification of polymer pyrolysis products greatly simplified since only signals from species originating from the sample cell are contained in the modulated mass spectrum. Details of the phase analysis of the modulated ion signals are discussed in the next section.

Evolution of pyrolysis products from the laser-irradiated sample can be detected independently from the mass filter signal by monitoring the outputs of an MKS Baratron gauge located in the sample cell, and an ionization pressure gauge located in the buffer chamber. The measured pressure profiles from both gauges were found to be identical. These gauges are total pressure sensors and provide information on the overall evolution rate of all volatile products in the sample cell. When tuned to a single ionic mass the mass filter acts as a partial pressure sensor and yields information on the evolution history of a given product. By simultaneously recording the total pressure and mass filter outputs it is possible to determine at which stage various products are created during laser pyrolysis of the sample. Knowledge of the relative formation rates of the different products provides important information on the chemical kinetics involved in pyrolysis reactions.

In electron impact ion sources the energy of the bombarding electrons is generally in the range 70–100 eV, well above the ionization potential of neutral species, where the ionization cross section is reasonably energy-independent and the ionization efficiency is at a maximum. However, these energies are also above the appearance potentials for formation of fragment ions. Uncertainties arise in identification of the precursor neutral species based on the observed ion spectra. These ambiguities can be removed by phase analysis of the modulated ion signals.

The measured phase lag for a given signal can be separated into components depending upon the neutral flight time $t_n = L/v_n$ over the chopper-to-ionizer distance L, and the ion transit time $t_i = d/v_i$ over the length d of the mass analyzer[8]. The total phase is given by

$$\phi = \phi_n + \phi_i = \omega(L/v_n + d/v_i) \tag{1}$$

where ω is the modulation frequency.

In the simplest approximation expressions for the mean inverse velocities ($\overline{1/v_n}$) and ($\overline{1/v_i}$) are proportional to the square root of the mass of the neutral, m_n, and ionic, m_i, species, respectively. For a constant sample source temperature eqn (1) can be rewritten as

$$\phi = Am_n^{1/2} + Bm_i^{1/2} \tag{2}$$

where A and B are constants containing the various instrumental parameters (e.g., chopping frequency, flight distances, ion energy) and in the case of A the molecular constants for the appropriate velocity distribution.

Since $m_n > m_i$ for fragment ions, while $m_n = m_i$ for parent ions, it is apparent from eqn (2) that at a given m/e value a signal due to a fragment ion will have a larger phase than that corresponding to a parent ion. The phase information can then be used to directly sort fragment ions from parent ions. In practice a known gas mixture, e.g., air plus benzene, is admitted to the system and from the measured phases of the known precursor species (H_2O^+, N_2^+, O_2^+, Ar^+ and $C_6H_6^+$) a calibration curve characteristic of parent ions is generated in a plot of ϕ vs. $m_i^{1/2}$ as shown by the solid line in Fig. 2. Ions whose phase values lie above this curve (e.g., N^+, $C_3H_3^+$) are associated, at least in part, with a neutral species of higher mass.

In addition to identifying a particular ion as a fragment, analysis of the phase measurements often enables the neutral precursor species to be determined. If a given fragment ion spectrum arises from a single parent molecule all the fragment ions will possess the same neutral phase component ϕ_n, and the fragment ion signal phases will follow a relationship of the form

$$\phi_{\text{frag}} = A' + Bm_i^{1/2} \tag{3}$$

where $A' =$ constant.

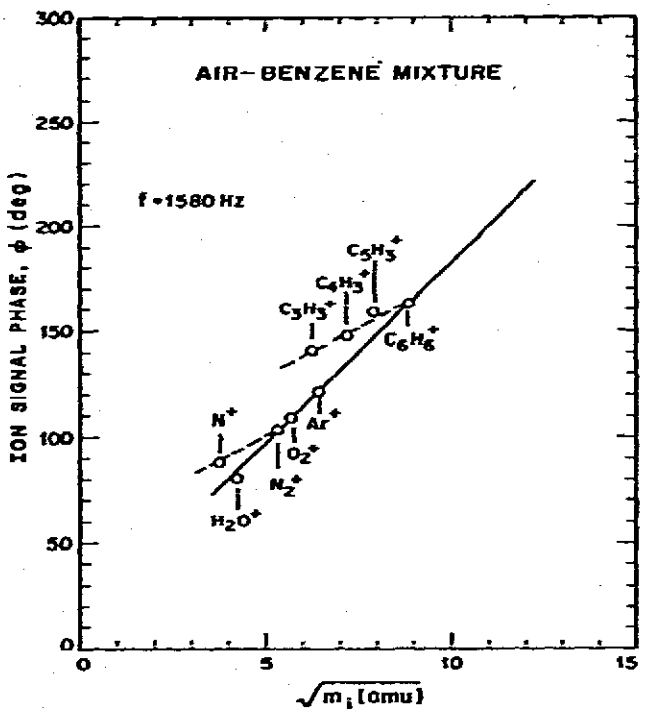

Fig. 2. Phase measurements for modulated ion signals from an air-benzene mixture: solid curve characteristic of parent ions; dashed curves characteristic of fragment ion spectrum from benzene and molecular nitrogen.

That is, in a plot of ϕ vs. $m_i^{1/2}$ the fragment ion phase values will lie on a straight line with slope B, shown by the dashed line of Fig. 2 for the $C_3H_3^+$, $C_4H_3^+$ and $C_5H_3^+$ fragments from benzene, which is shallower than the line characteristic of parent ions (slope $= A + B$, from eqn (2)). The dashed and solid lines will intersect at a point corresponding to the m_i value of the parent molecule. Contributions to a particular fragment ion by a second lower molecular-weight parent molecule will proportionately decrease the overall fragment ion phase value; a second parent of higher molecular weight, on the other hand, will displace the fragment ion phase to higher values. Obviously, as the number of neutral molecules yielding the same fragment ion increases the amount of information contained in the phase measurement decreases. However, the basic capability of discriminating purely primary ions from those arising from various dissociative ionization processes still provides an important simplification to the interpretation of complex spectra.

RESULTS

Rigid poly (vinyl chloride)

Laser target samples of rigid PVC, containing no plasticizer or stabilizer additives, were obtained by hot pressing the pure resin powder at 180°C to form

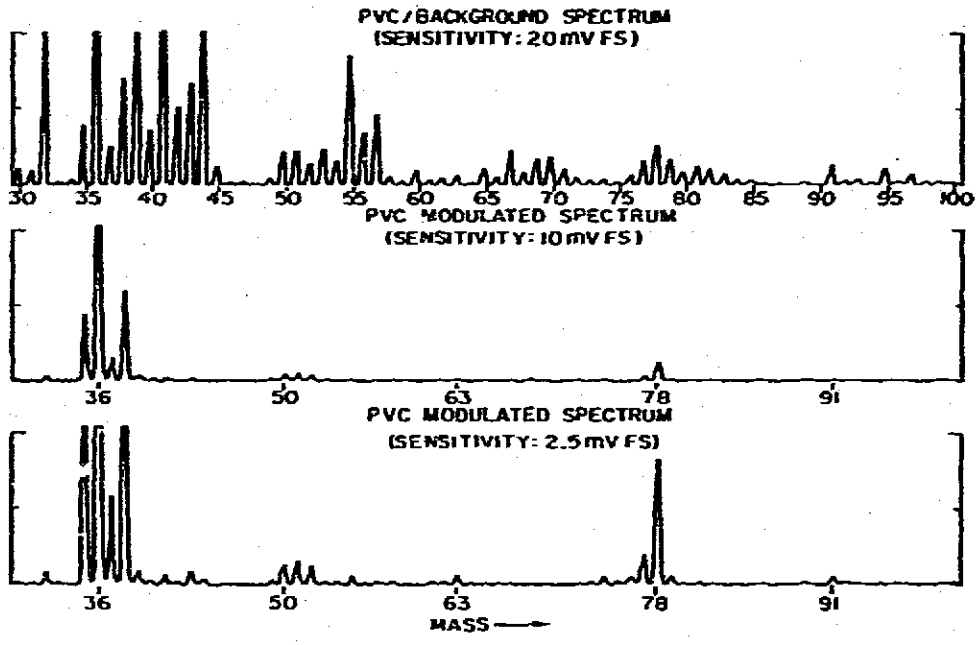

Fig. 3. Simultaneous "d.c." and modulated mass spectra from laser-irradiated rigid PVC.

0.5 mm thick disks. Simultaneous recordings of the total ion signal and the modulated component only are presented in the mass spectra of Fig. 3. The upper scan is the combined spectrum of the laser-vaporized species from the PVC sample and of the residual gases present in the analysis chamber. However, only the PVC pyrolysis products which form the modulated molecular beam appear in the spectra of the lower two traces. Rejection of the unmodulated signal contributions from the residual gas is clearly evident.

The modulated mass spectrum of the volatile pyrolysis products is relatively simple and is dominated by the evolution of hydrogen chloride ($m/e = 35$–38). The major hydrocarbon species evolved is benzene ($m/e = 78$) with a relative intensity approximately a factor of 10 less than the HCl signal. A small amount of toluene ($C_6H_5CH_3$), identified by the peaks at $m/e = 91$ and 92, is also present in the laser vaporized plume. Heavier aromatic species are also observed, e.g., naphthalene ($m/e = 128$) and methylnaphthalene ($m/e = 142$), but at much lower intensities than even the toluene signal[9] and will not be discussed further here.

Phase analysis of the modulated ion signals, performed in Fig. 4, definitely establishes that the peaks at $m/e = 39$, 50–53 and 63 are fragment ions resulting from dissociative ionization of benzene. This analysis also confirms the identification of the $m/e = 36$, 78 and 92 ions as primary ions. However, since the accuracy of the phase measurements is approximately $\pm 2°$, an upper limit is placed on the mass of the largest fragment which can be distinguished from a parent species. Under the experimental conditions of Fig. 4, for example, the mass resolution is $m/\Delta m = 25$. That is, the $C_5H_3^+$ fragment ($m/e = 63$) from

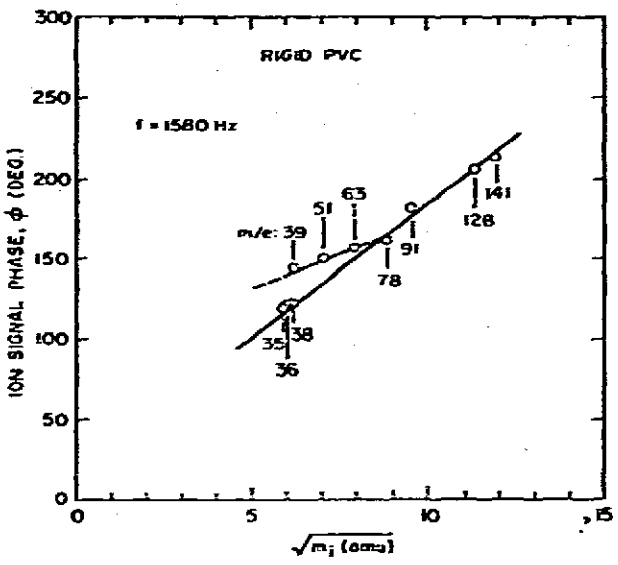

Fig. 4. Phase measurements for modulated ion signals from rigid PVC. Correlation with parent ions occurs for signals at $m/e = 36$ and 38 (hydrogen chloride), 78 (benzene), 91 (toluene), 128 (napthalene) and 141 (methylnapthalene). Signals at $m/e = 39$, 51 and 63 ($C_3H_3^+$, $C_4H_3^+$, $C_5H_3^+$) correlate with phase values of fragment ions from benzene.

benzene can be easily identified from its phase (see Fig. 4); whereas the $C_6H_3^+$ fragment ($m/e = 75$) is near the resolution limit and, within experimental error, its phase would be indistinguishable from that of a parent ion. In such cases information on isotopic abundance ratios and fragment ion relative intensities is required for a complete analysis.

The relative vaporization rates of the three major products released from PVC are illustrated in Figs. 5a–c. In each case the upper trace represents the total pressure pulse due to all gases evolved from the polymer substrate, and the lower trace is the partial pressure (mass filter signal) of the individual species. Time-resolved signals were obtained by sequentially tuning the mass analyzer to each specific ion peak and irradiating a different portion of the sample with the laser beam for a set time interval. The partial pressures of HCl, benzene and toluene all track the total pressure profile. Several degradation reactions resulting in the formation of higher molecular-weight organic products thus occur simultaneously with the dehydrochlorination of PVC. Measurements by Kleineberg et al.[10], using combined thermogravimetric–mass spectrometric methods, and by Chang and Salovey[11], using a gas chromatography–mass spectrometric technique, confirm the concurrent evolution of HCl and benzene from PVC in the temperature range ~250–400 °C.

Water vapor is also detected in the laser-vaporized products from PVC. However, examination of the time-resolved water signal shown in Fig. 6 indicates that it is not a true decomposition product. Rather, the large initial release of

water is associated with adsorbed species and the subsequent sporadic bursts are most likely due to vaporization of occluded water as the sample volume is heated.

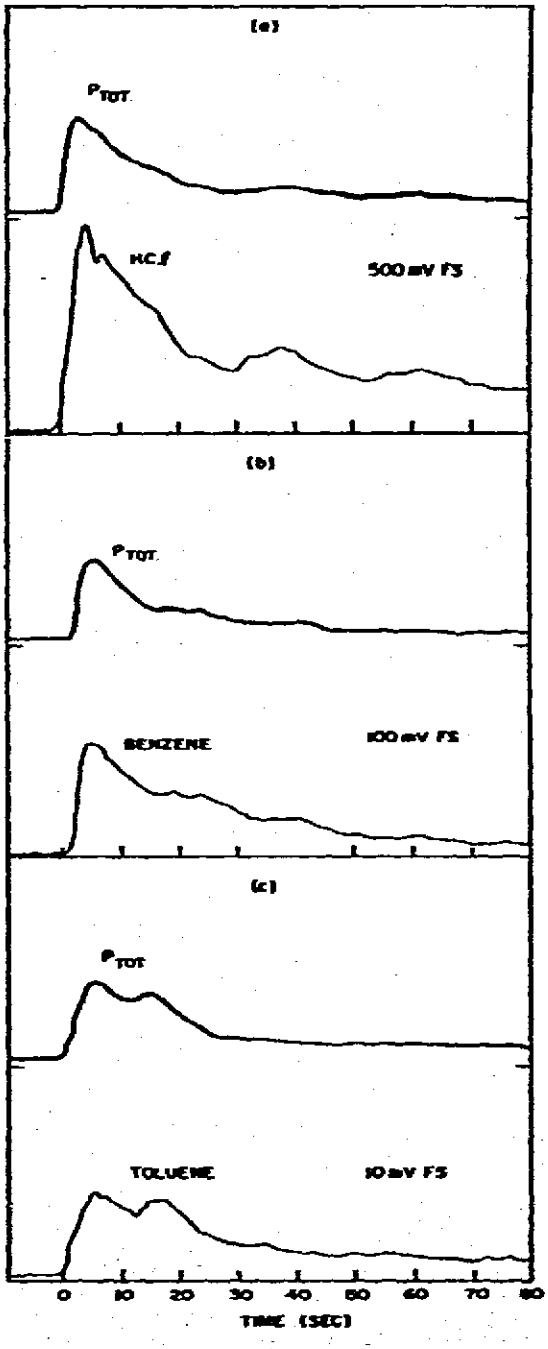

Fig. 5. Evolution profiles for laser vaporized species from rigid PVC. (a) Hydrogen chloride; (b) benzene; (c) toluene.

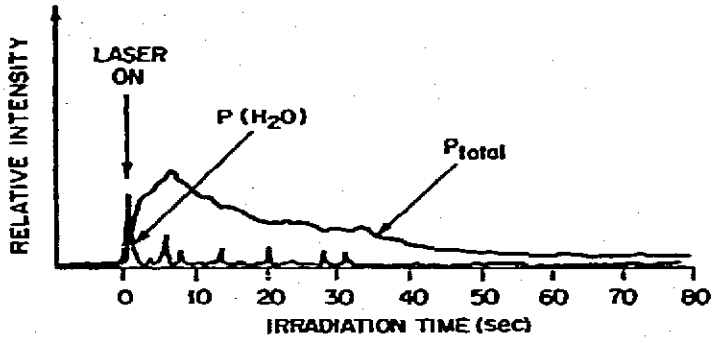

Fig. 6. Desorption of water vapor from rigid PVC sample.

The early stages of PVC degradation were investigated by monitoring product evolution at increased detection sensitivities. Initial evolution of the various species occurs in distinctly separate stages as shown in Fig. 7. Evolution of HCl is observed approximately 7 sec prior to the initial detection of benzene evolution. During this interval the $m/e = 36$ modulated HCl ion signal gradually increases to approximately 0.1% of its ultimate maximum value. These results are supported by the measurements of Chang and Salovey[11] which indicate that as the pyrolysis temperature is increased, first HCl, then benzene, and finally toluene and heavier aromatics are formed.

Although the detailed mechanism of dehydrochlorination is still unsettled[12], the thermal degradation of PVC can be characterized by unzipping of successive HCl units from the polymer chain[13]. This results in the formation of conjugated double bond sequences in the polymer,

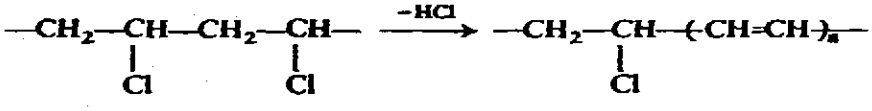

(4)

Formation of benzene can be accounted for by cyclization of triene units from such polyene sequences[11, 14, 15]

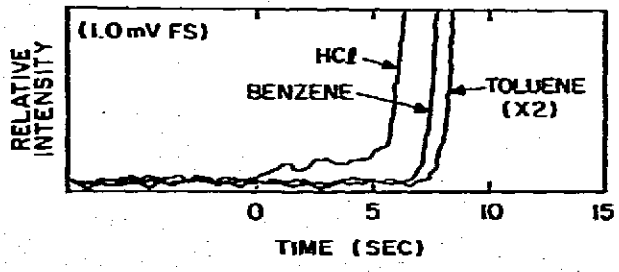

Fig. 7. Initial evolution characteristics for hydrogen chloride, benzene and toluene from rigid PVC irradiated with a focused laser beam.

Plasticized poly (vinyl chloride)

Additives can significantly affect both the composition and the evolution rate of the volatile polymer decomposition products. Results from laser irradiation of a PVC formulation containing a standard phthalate plasticizer are shown in the modulated mass spectra of Fig. 8. The volatile products are still dominated by HCl from the PVC resin. However, vaporization and decomposition of the plasticizer species results in the appearance of a mass peak at virtually every value of m/e out to $m/e = 100$ (compare with the rigid PVC spectra of Fig. 3). For $m/e > 100$ the spectra for rigid and plasticized PVC are very similar, except for peaks at $m/e = 148$ and 149 which are characteristic of the phthalate-plasticizer.

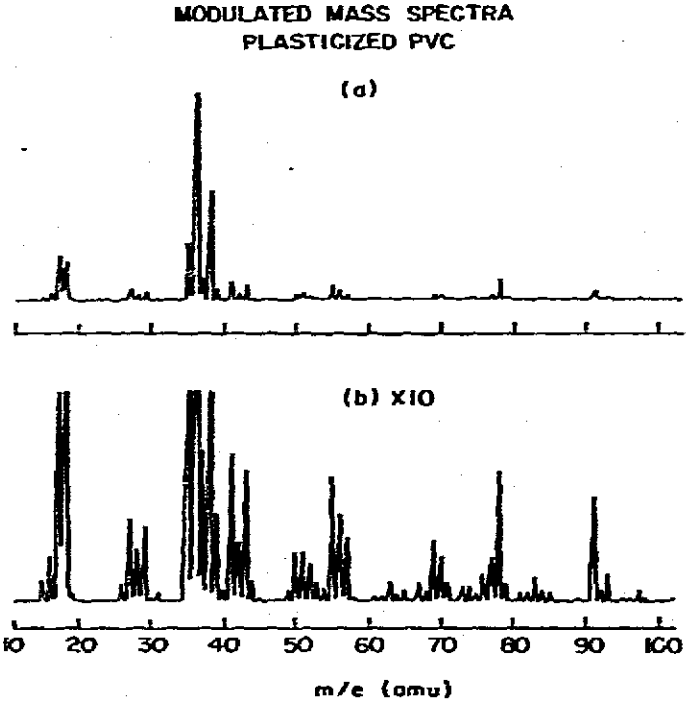

Fig. 8. Modulated mass spectra from plasticized PVC.

The vaporization characteristics of HCl, benzene and toluene from the plasticized PVC sample are shown in Fig. 9. Evolution profiles for HCl and benzene are similar to those observed for rigid PVC and indicate that these species originate from decomposition of the PVC resin as discussed earlier. However, the toluene signal exhibits a radically different time dependence. Toluene, or a species having a similar m/e ratio, appears to be formed from an additional source during the latter decomposition stages of the plasticized PVC sample.

Effects of flame retardant additives on polymer pyrolysis reactions were examined with a plasticized PVC composition containing 3 phr (parts per hundred

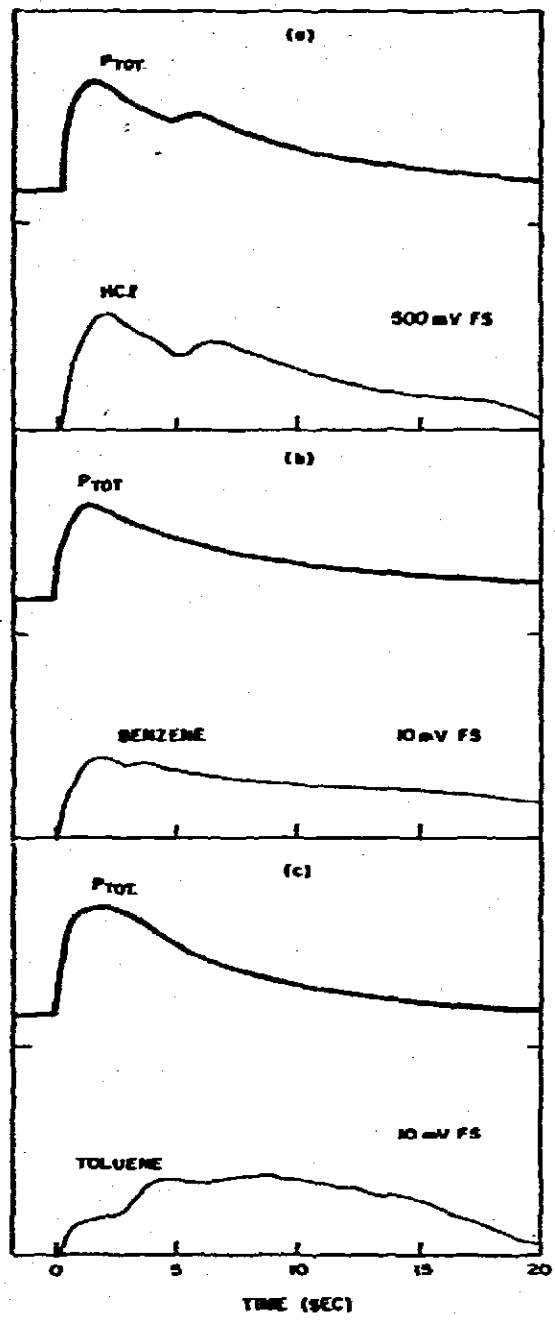

Fig. 9. Evolution profiles for laser vaporized species from plasticized PVC. (a) Hydrogen chloride; (b) benzene; (c) toluene.

resin) of antimony trioxide, Sb_2O_3. It is well known that a synergistic flame retardancy effect is observed when Sb_2O_3 is incorporated into organic halide materials such as PVC. The detailed thermochemistry involved, however, has only recently begun to be investigated[16–18]. Proposed mechanisms center on the interaction of HCl, evolved from the polymer substrate, with Sb_2O_3 to form volatile $SbCl_3$ species which are transported to the flame zone[19]. The modulated mass spectrum of the laser pyrolysis products presented in Fig. 10 provides the first direct evidence for the production of volatile $SbCl_3$ during the thermal decomposition of an actual Sb_2O_3–PVC polymer formulation.

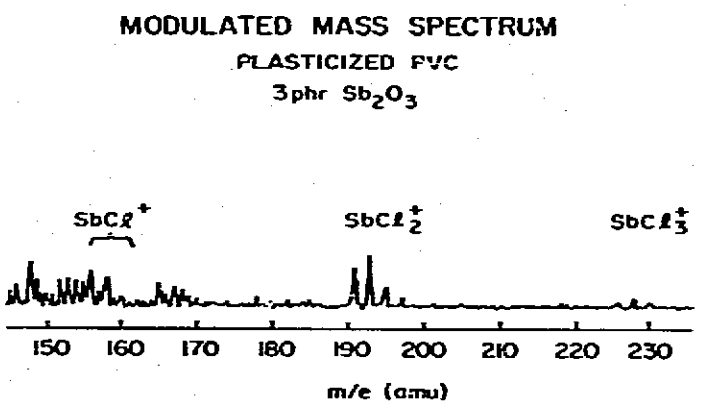

Fig. 10. Modulated mass spectrum from plasticized PVC containing 3 phr Sb_2O_3 flame retardant additive.

Recent measurements[18] on the laser pyrolysis of rigid PVC in the presence of a small amount of SB_2O_3 powder indicates that the evolution of HCl is greatly moderated by the production of $SbCl_3$ as shown in Fig. 11a. The dashed curves represent the corresponding pressure and species profiles obtained during laser vaporization of rigid PVC in the absence of Sb_2O_3. HCl evolution is lower by approximately a factor of ten from the maximum level observed without the flame retardant additive. The absence of a burst-like character in the evolution of water vapor from the Sb_2O_3–PVC system (Fig. 11b) indicates that in this case H_2O is a true reaction product and not simply an adsorbed species as in the case of rigid PVC alone.

Information on the extent of the reaction between HCl and Sb_2O_3 can be obtained from the phase measurements of the major ions observed in the Sb_2O_3–PVC modulated mass spectrum. These values are shown in Fig. 12 from which the primary ions corresponding to water vapor, HCl, benzene, toluene and $SbCl_3$ are readily identified. Also apparent is the definite phase relationship exhibited by the fragment ions of $SbCl_3$. Of particular note is the phase difference $\Delta\phi \sim 25°$ observed between the $^{35}Cl^+$ and $H^{35}Cl^+$ ions; a similar difference is measured between the relative phases of the $^{37}Cl^+$ and $H^{37}Cl^+$ ions. Clearly, the con-

tribution to the Cl^+ signals due to dissociative ionization of $SbCl_3$ completely dominates that arising from fragmentation of HCl indicating a rather extensive reaction between HCl and Sb_2O_3.

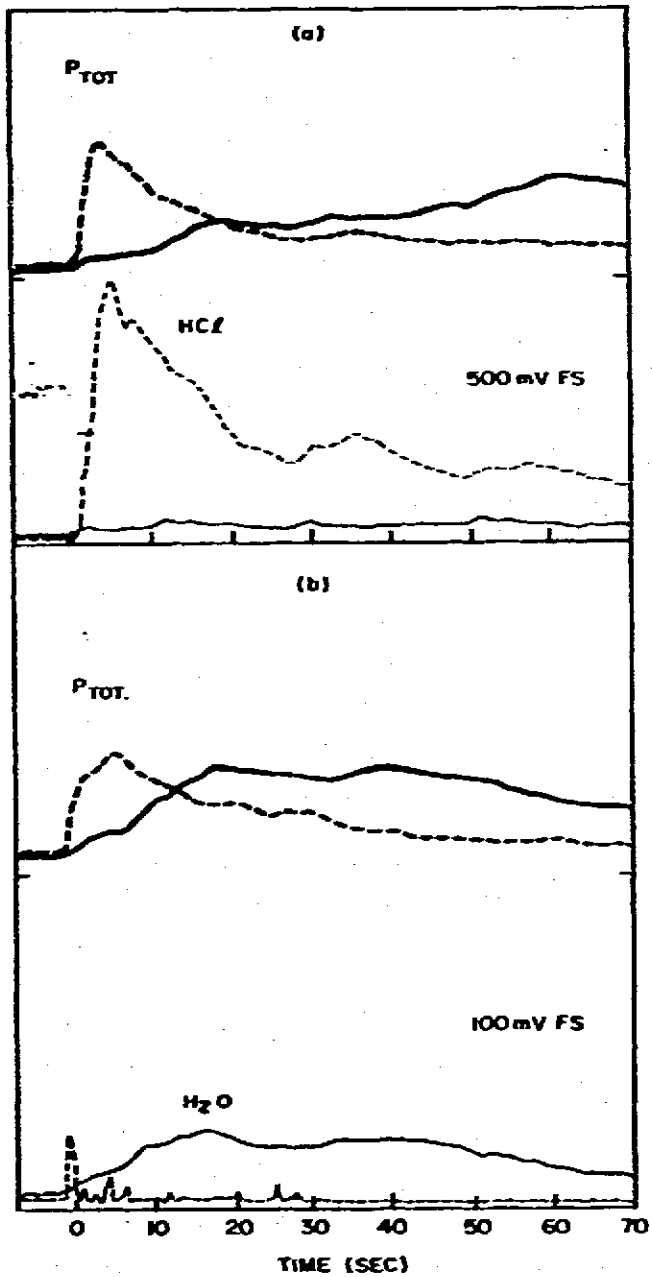

Fig. 11. Evolution profiles for laser vaporized species and reaction, products from Sb_2O_3–PVC system (solid curves). (a) Hydrogen chloride; (b) water vapor. The dashed curves represent the corresponding profiles from rigid PVC in the absence of Sb_2O_3.

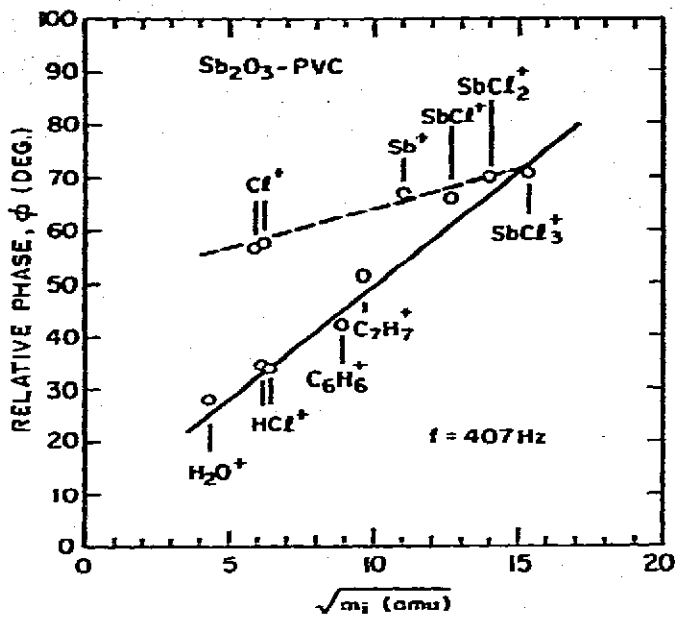

Fig. 12. Phase measurements for modulated ion signals from Sb_2O_3–PVC system. Signals at $m/e = 35$ and 37 (Cl^+) are dominated by dissociative ionization from $SbCl_3$ rather than by fragmentation of HCl (compare with Fig. 4).

Polyoxymethylene copolymer

Polyoxymethylene materials of increased thermal stability are obtained by copolymerization of trioxane with small amounts of cyclic ethers such as ethylene oxide[20–22]. The regular $-CH_2O-$ polyoxymethylene structure is interrupted at various points along the polymer chain by $-CH_2CH_2O-$ units. Introduction of carbon–carbon linkages in the copolymer results in the formation of ether–alcohol groups at the chain ends which account for the greater degree of thermal stability. Samples for laser probe analysis were prepared directly from the resin pellet stock.

The laser pyrolysis products are dominated by monomer formaldehyde species as shown in the modulated mass spectra of Fig. 13. However, trace ion signals from other species are apparent in the higher sensitivity spectral scans. The highest ion mass for which a signal is observed occurs at $m/e = 104$; scans were performed out to $m/e = 300$.

Sorting of the observed ion signals according to their phases is presented in Fig. 14. Although the $m/e = 31$ and 61 ions are the most intense of the minor signals, their phase values clearly indicate that they are fragment ions—as are the ions at $m/e = 12$, 29 and 91. On the other hand, the phase analysis indicates that the signals at $m/e = 30$, 73 and 89 are associated with parent ions. An intermediate situation is presented by the $m/e = 45$ signal. While its measured phase is greater than that characteristic of a parent ion, it is somewhat lower than that corresponding solely to a fragment ion from any of the known higher molecular-weight parent ions. Thus, as discussed for the general case in the section on

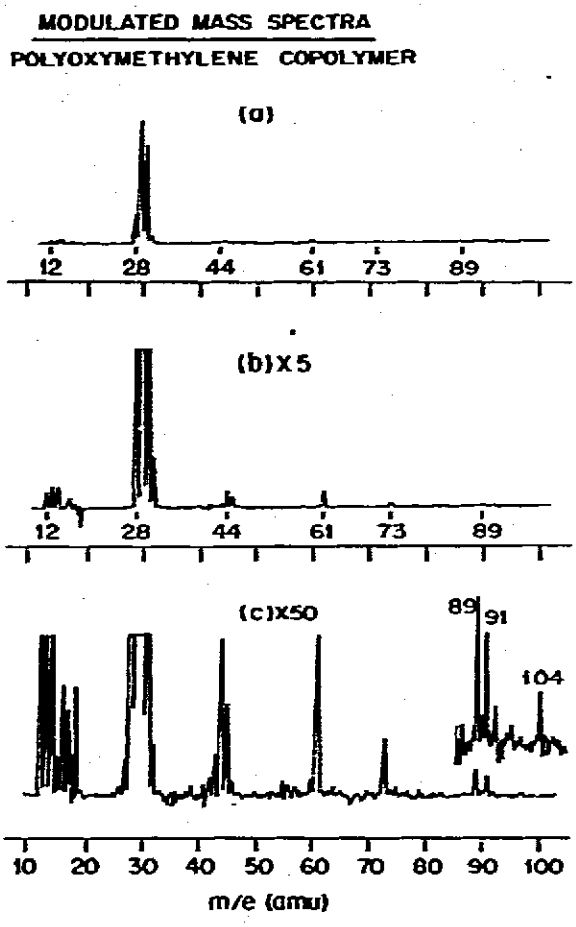

Fig. 13. Modulated mass spectra from trioxane–ethylene oxide copolymer.

phase spectrometry, at least two precursors (a low molecular-weight species, $m/e \sim 45$, and a higher molecular-weight component, $m/e \sim 73$) appear to make significant contributions to the $m/e = 45$ ion signal.

Using the above information on the amplitude and phase of the modulated ion signals the trace species are readily identified and correlated with the structure of the polyoxymethylene copolymer as illustrated in Fig. 15. The $m/e = 31$, 61 and 89 ion phases correlate well with the fragment ion spectrum from trioxane ($m/e = 90$) molecular species. However, since their relative phases differ by $\Delta\phi = 4°$ the $m/e = 91$ signal is clearly not associated with the same neutral species as the $m/e = 89$ ion. The only peak at higher mass numbers, as seen in the inset of Fig. 13c, is that observed at $m/e = 104$. The good agreement between the measured $m/e = 91$ phase and the value expected for a fragment from $m/e = 104$ confirms that this is indeed the precursor species, which can be identified as 1,3,5-trioxepane. The low amplitude of the $m/e = 104$ signal prevented a reliable measurement of its phase.

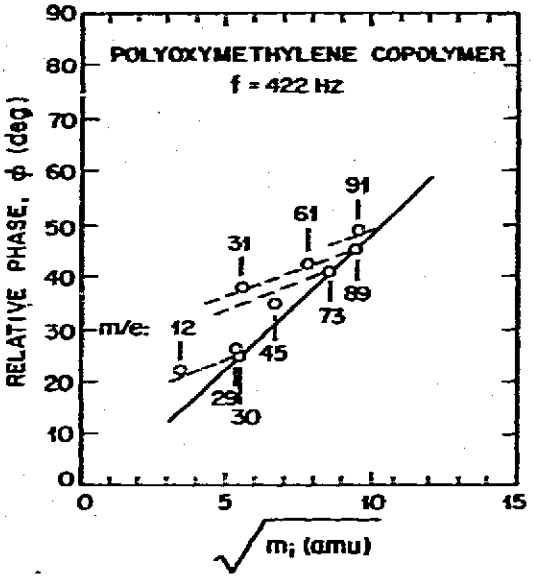

Fig. 14. Phase measurements for modulated ion signals from trioxane-ethylene oxide copolymer. Ions at $m/e = 30$, 73 and 89 correlate with formaldehyde, 1,3-dioxolane and trioxane neutral species, respectively. The $m/e = 91$ fragment ion correlates with the neutral precursor 1,3,5-trioxepane ($m/e = 104$).

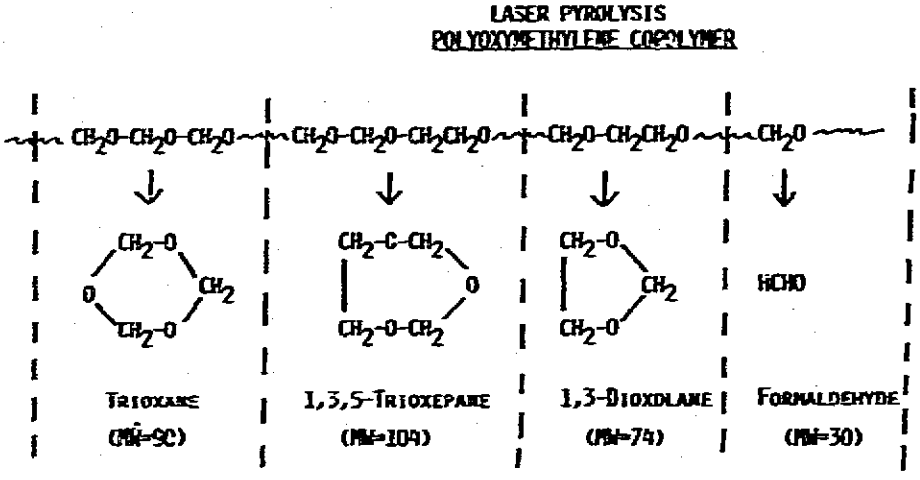

Fig. 15. Schematic representation of the laser-induced cleavage of polyoxymethylene copolymer into the observed neutral fragments.

Since the measured phase for the $m/e = 73$ signal lies near the line characteristic of parent ions it can be identified as the $C_3H_5O_2^+$ ion originating from 1,3-dioxolane*. Although the major contribution to the $m/e = 45$ ion also appears

*Experiments with trioxane and dioxolane gas indicate that the parent ion M^+ is produced with low yield, e.g., in both cases the relative intensity of M^+ is less than a tenth of that observed for the $(M-1)^+$ fragment ion[23].

to be dissociative ionization of dioxolane, the phase measurements indicate that small amounts of ethyl alcohol may also be produced[24]. Upon ionization C_2H_5OH yields the (M–H) fragment ($m/e=45$) as a major ion species. Ion signal contributions from this fragment would possess a relative phase lag approximately 6° less than the corresponding m/e fragment from dioxolane (CHO_2^+) resulting in the intermediate net value observed in Fig. 14 for the $m/e=45$ ion signal phase.

Although less pronounced, a similar situation holds for the $m/e=29$ ion which is the most intense ion in the formaldehyde spectrum. Its measured phase is consistently 1.5–2.0° greater than that observed for the $m/e=30$ parent ion from formaldehyde. This indicates that contributions to the $m/e=29$ signal from higher molecular-weight species are significant—even though these latter species are present in the molecular beam at much lower concentrations than formaldehyde. For example, the $m/e=29$ CHO^+ species is a common fragment from all the pyrolysis products listed in Fig. 15.

Finally, accurate phase measurements for the $m/e=44$ ion could not be obtained due to high noise levels in the modulated signal arising from the combination of a relatively low beam signal and a large "d.c." background signal. However, the $m/e=44$ peak is most likely associated with the ethylene oxide copolymer species either arising from the evolution of CO_2[24] or the monomer species itself.

Polyether ester copolymer

Segmented polyether ester block copolymers have recently been developed for use as thermoplastic elastomers[25,26]. The copolymer structure consists of alternating sequences of amorphous soft segments responsible for the elastomeric nature of the polymer, and crystalline hard segments which provide crosslinking[27]. Crystallizable tetramethylene terephthalate units form the hard blocks,

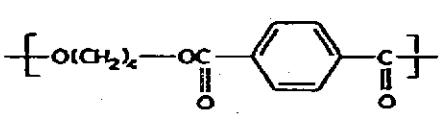

(5)

and the soft-segment homopolymer is poly(tetramethylene ether) glycol terephthalate,

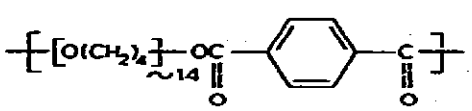

(6)

which is a gum-like substance. Disk samples for analysis were prepared by compression molding of the polymer material which was obtained in pellet form.

The modulated mass spectrum of the laser pyrolysis products from the polyester copolymer is shown in Fig. 16. The highest mass peak observed in this spectrum occurs at $m/e=78$. Higher sensitivity scans out to $m/e=300$ reveal the presence of two additional peaks at $m/e=105$ and 122 with signal intensities less than 5% of the $m/e=72$ signal. No other high mass species are observed. This

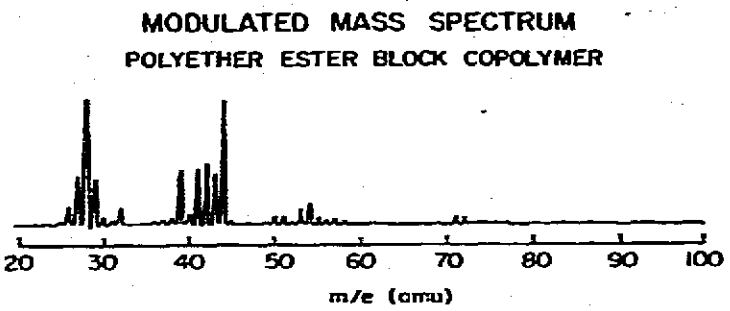

Fig. 16. Modulated mass spectrum from polyether ester block copolymer.

rules out the vaporization of monomer species from the tetramethylene terephthalate hard segments ($m/e = 220$) of the copolymer; and also polymer fragments of tetramethylene ether, $[O(CH_2)_4]_n$, from the soft segments.

Measured phase lags for the ion signals are presented in Fig. 17. It is immediately obvious that the bulk of the ions observed in the modulated spectrum of Fig. 16 possess signal phases characteristic of fragments from a precursor spe-

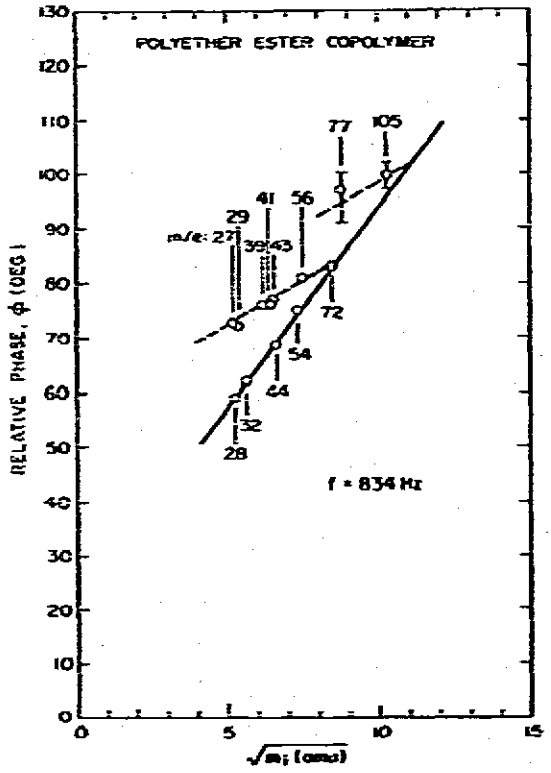

Fig. 17. Phase measurements for modulated ion signals from polyether ester copolymer. The $m/e = 54$ parent ion (1,3-butadiene) is easily picked out of the extensive fragment ion spectrum of tetrahydrofuran ($m/e = 72$). The $m/e = 77$ and 105 fragment ions correlate with the neutral precursor benzoic acid ($m/e = 122$).

cies at $m/e = 72$. From the structure of the copolymer given in eqns (5) and (6) it is clear that the $m/e = 72$ peak can be attributed to volatile tetramethylene oxide, i.e., tetrahydrofuran (THF), which is a heterocyclic compound,

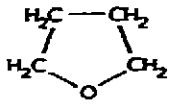

This assignment is substantiated by the known fragmentation pattern of THF[23] which lists the parent ion ($m/e = 72$) and the $m/e = 71$ fragment as appearing with approximately equal intensities.

Based solely on the mass spectral data of Fig. 16 the peaks at $m/e = 50$–59 all appear to be minor fragment ions; no readily distinguishing features are evident for any one peak. However, the phase measurements indicate a distinct phase difference of $\Delta\phi = 6°$ between the $m/e = 54$ and 56 signals. Although $m/e = 56$ is clearly a fragment ion of THF, the $m/e = 54$ signal has a phase value characteristic of a parent ion. This indicates that the polyester polymer pyrolysis reactions result in the direct formation of conjugated dienes such as 1,3-butadiene (CH_2=CH–CH=CH_2). Formation of similar polyene structures is also observed in the laser pyrolysis of PVC as discussed earlier. This example demonstrates the power of the phase spectrometry technique to dig parent ion signals out of a complicated fragment ion spectrum.

The phase relationship of the $m/e = 77$ and 105 ions strongly suggest that they are fragments of the $m/e = 122$ parent ion, although accurate phase measurements for these ions are difficult due to their low signal intensities. Attempts to increase the signal intensities resulted in significant pressure variations in the sample cell during the time required for a phase measurement. Vasile et al.[28] have shown that such variations affect the observed phase values of the modulated ion signals. The observed spread in measured phase lags for the $m/e = 77$ and 105 ions is indicated by the vertical bars in Fig. 17. A possible assignment of the neutral pyrolysis product corresponding to $m/e = 122$ is benzoic acid,

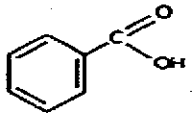

in which it is known[29,30] that the carbonyl group exhibits ready cleavage of the bonds to its substituents to yield the parent minus OH ($m/e = 105$) and the parent minus COOH ($m/e = 77$) ions as the most intense peaks.

Finally, the relatively large phase differences observed for $\phi(27)$–$\phi(28)$ and $\phi(43)$–$\phi(44)$ establish that the $m/e = 28$ and 44 ions are not fragment species from organic molecules. Rather, their phase values lie on the line characteristic of parent ions and indicate the presence of CO and CO_2 species in the laser-vaporized plume.

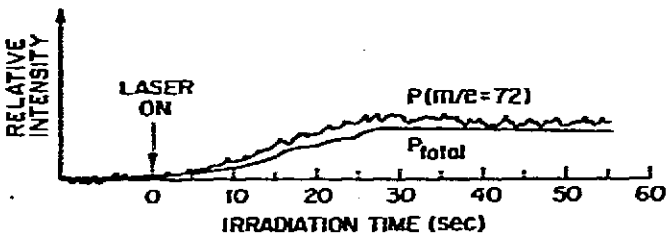

Fig. 18. Evolution profile for laser vaporized tetrahydrofuran species ($m/e = 72$) from the polyether ester copolymer.

Evolution of THF species from the polyester copolymer during irradiation of a single pellet sample with a focused laser beam is shown in Fig. 18. The pressure–time characteristics depicted in this figure actually represent depth profiles for the copolymer sample. As the sample is initially irradiated the total pressure gradually increases and then remains constant as the laser beam penetrates the sample. Sample penetration is illustrated in Fig. 19 by photomicrographs of the sample surface and cross-section. Depth profiles of the various vaporization products are similar indicating a uniform sample composition. This technique promises to be a valuable analytical tool for the study of composite materials—e.g., determination of composition variations, investigation of additive dispersion in polymer formulations, etc.

CONCLUSION

Laser probe analysis complements conventional thermal analysis techniques and offers several unique capabilities. Only the sample itself is heated, thus eliminating interfering reactions which could otherwise occur at the hot surfaces of the sample cell or with contaminant species liberated by cell components at elevated temperatures. Precise sample areas can be probed by focusing the laser radiation to a small spot. Use of molecular beam sampling techniques and mass analysis permits direct sampling of the pyrolysis products as they evolve from the cell. Analysis of the phase information contained in the modulated ion signals to discriminate between parent ions of pyrolysis products and those resulting from fragmentation processes in the ionization chamber has been successfully demonstrated for several complex polymer systems. In many cases the neutral precursor of a given fragment ion was determined directly from the phase measurements. Information was obtained on the identity and relative vaporization rates of the volatile species. The time-resolved mass spectral data enabled adsorbed species to be distinguished from true polymer decomposition products and provided information on the dynamic behavior of the decomposition processes. Further development will involve detection of free radicals and other reactive species as they evolve directly from the polymer surface. Information on the identity and evolution characteristics of these species is important in determining the detailed mechanisms involved in polymer pyrolysis.

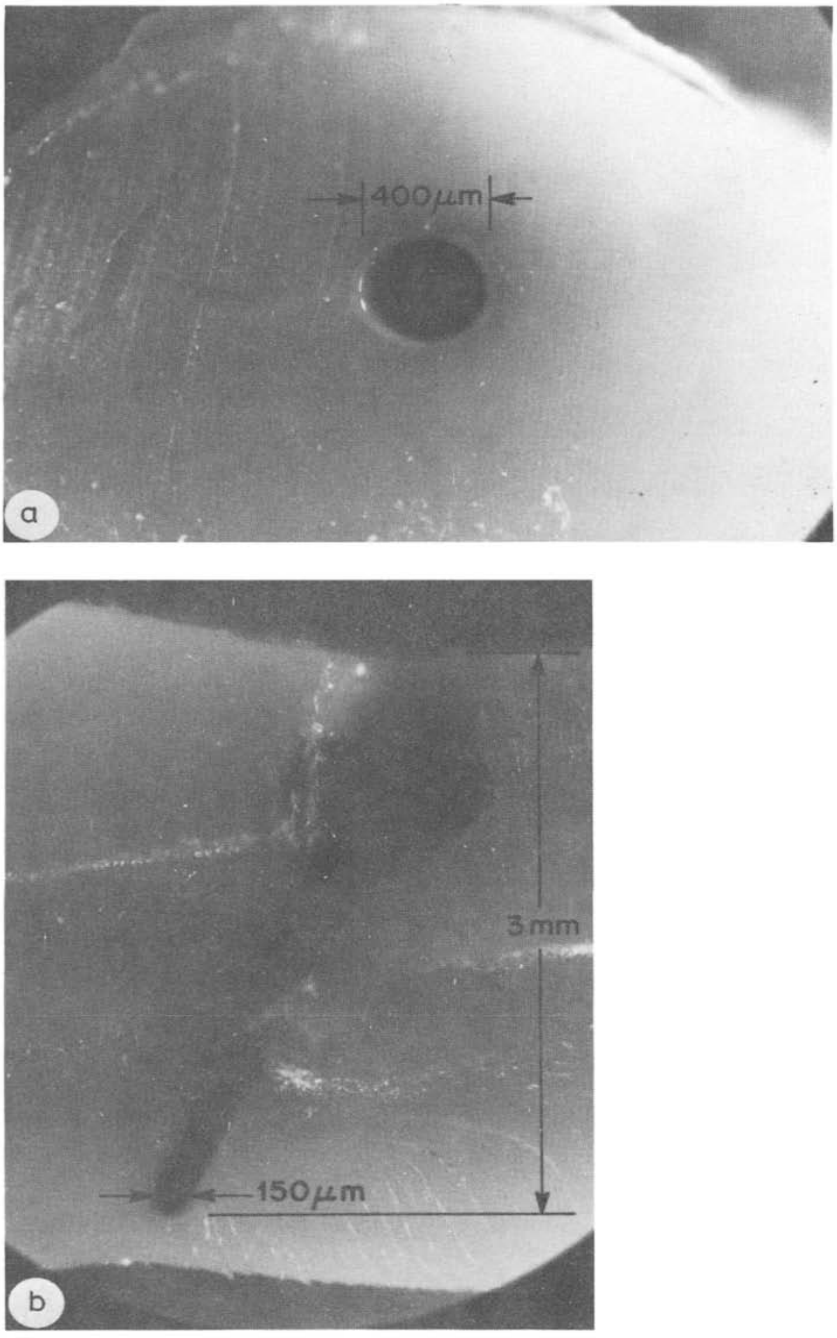

Fig. 19. Photomicrographs of a single pellet sample of the polyether ester copolymer: (a) surface view illustrating 400μm hole bored by focused laser beam; (b) cross-section view depicting laser beam penetration to a sample depth of 3 mm (150μm min. diam.).

REFERENCES

1 H. L. Friedman, *J. Appl. Polym. Sci.*, 9 (1965) 651.
2 K. A. Lincoln, *Anal. Chem.*, 37 (1965) 541.
3 R. E. Honig, in H. J. Schwarz and H. Hora (Eds.), *Laser Interaction and Related Phenomena*, Plenum, New York, 1971, p. 85.
4 B. E. Knox, in D. Price (Ed.), *Dynamic Mass Spectrometry*, Vol. 2, Heyden & Son, London, 1972, p. 61.
5 W. K. Joy and B. G. Reuben, in D. Price and J. E. Williams (Eds.), *Dynamic Mass Spectrometry*, Vol. 1, Heyden & Son, London, 1970, p. 183.
6 F. Hillenkamp, E. Unsöld, R. Kaufman and R. Nitsche, *Nature*, 256 (1975) 119.
7 K. R. Thompson, *Anal. Chem.*, 48 (1976) 696.
8 W. L. Fite, *Int. J. Mass Spectrom. Ion Phys.*, 16 (1975) 109.
9 R. M. Lum, *J. Appl. Polym. Sci.*, 20 (1976) 1635.
10 G. A. Kleineberg, D. L. Geiger and W. T. Gormley, *Technical Report AMRL-TR-73-88*, Aerospace Medical Research Laboratory, Wright-Patterson Air Force Base, Ohio, 1973.
11 E. P. Chang and R. Salovey, *J. Polym. Sci., Polym. Chem. Ed.*, 12 (1974) 2927.
12 D. Braun, in G. Geuskens (Ed.), *Degradation and Stabilization of Polymers*, Halsted Press, 1975, p. 23.
13 W. C. Geddes, *Rubber Chem. Technol.*, 40 (1967) 177.
14 R. R. Stromberg, S. Straus and B. G. Achhammer, *J. Polym. Sci.*, 35 (1959) 355.
15 G. A. Rasuvaev, L. S. Troitskaya and B. B. Troitskii, *J. Polym. Sci.*, 9 (1971) 2673.
16 J. J. Pitts, P. H. Scott and D. G. Powell, *J. Cell. Plast.*, 6 (1970) 35.
17 J. W. Hastie, *J. Res. NBS*, 77A (1973) 733.
18 R. M. Lum, *J. Polym. Sci., Chem. Ed.*, (1977) in press.
19 J. W. Hastie, *Combust. Flame*, 21 (1973) 49.
20 W. Kern, H. Cherdron and V. Jaacks, *Angew. Chem.*, 73 (1961) 177.
21 K. H. Burg, E. Fischer and K. Weissermel, *Makromol. Chem.*, 103 (1967) 268.
22 P. G. Kelleher and B. D. Gesner, *Polym. Eng. Sci.*, 10 (1970) 38.
23 A. Cornu and R. Massot, *Compilation of Mass Spectral Data*, Vol. 1, Heyden & Son, New York, N.Y., 1975.
24 S. L. Madorsky and S. Straus, *J. Polym. Sci.*, 36 (1959) 183.
25 W. K. Witsiepe, *ACS Polym. Prepr.*, 13 (1972) 588.
26 G. K. Hoeschele, *Polym. Eng. Sci.*, 14 (1974) 848.
27 W. H. Buck and R. J. Cella, *ACS Polym. Prepr.*, 14 (1973) 98.
28 M. J. Vasile, F. A. Stevie and W. E. Falconer, *Int. J. Mass Spectrom. Ion Phys.*, 17 (1975) 195.
29 F. W. McLafferty and R. S. Gohlke, *Anal. Chem.*, 31 (1959) 2076.
30 J. H. Benyon, B. E. Job and A. E. Williams, *Z. Naturforsch.*, 20A (1965) 883.